MIET
NATIONAL RESEARCH UNIVERSITY OF ELECTRONIC TECHNOLOGY

Nano Innovation 2020
Rome, 15-18 September
Conference & Exhibition

Mono- and bimetallic nanoparticles in sensor and catalysis devices

Section: Nanomaterials for sensoristic applications

Sergey Dubkov, Ph.D.
sv.dubkov@gmail.com

Historical Note

Zelenograd foundation date – 1958

MIET foundation date - 1965

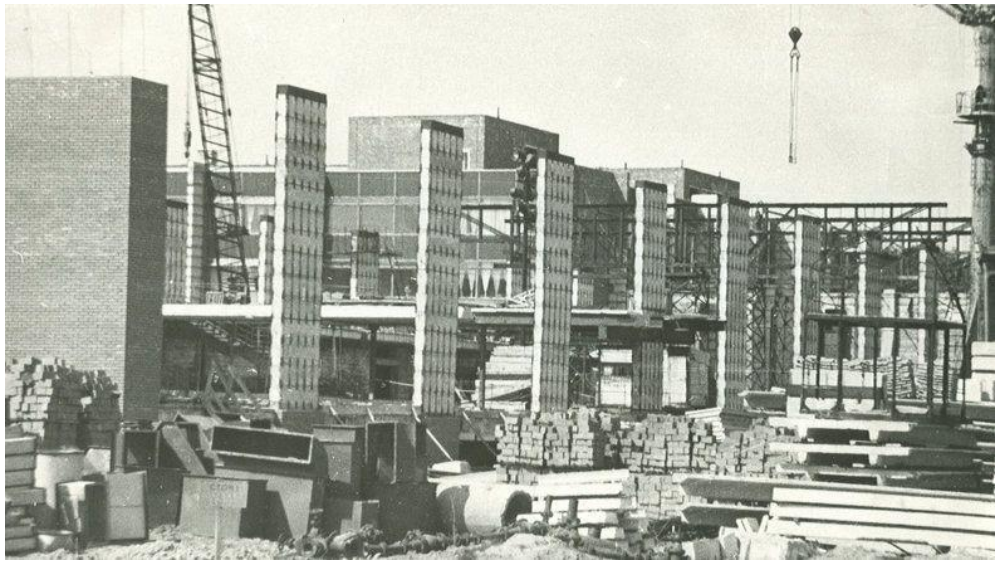

USSR Minister of Electronic Industry - Alexander Shokin

Topic

Zelenograd

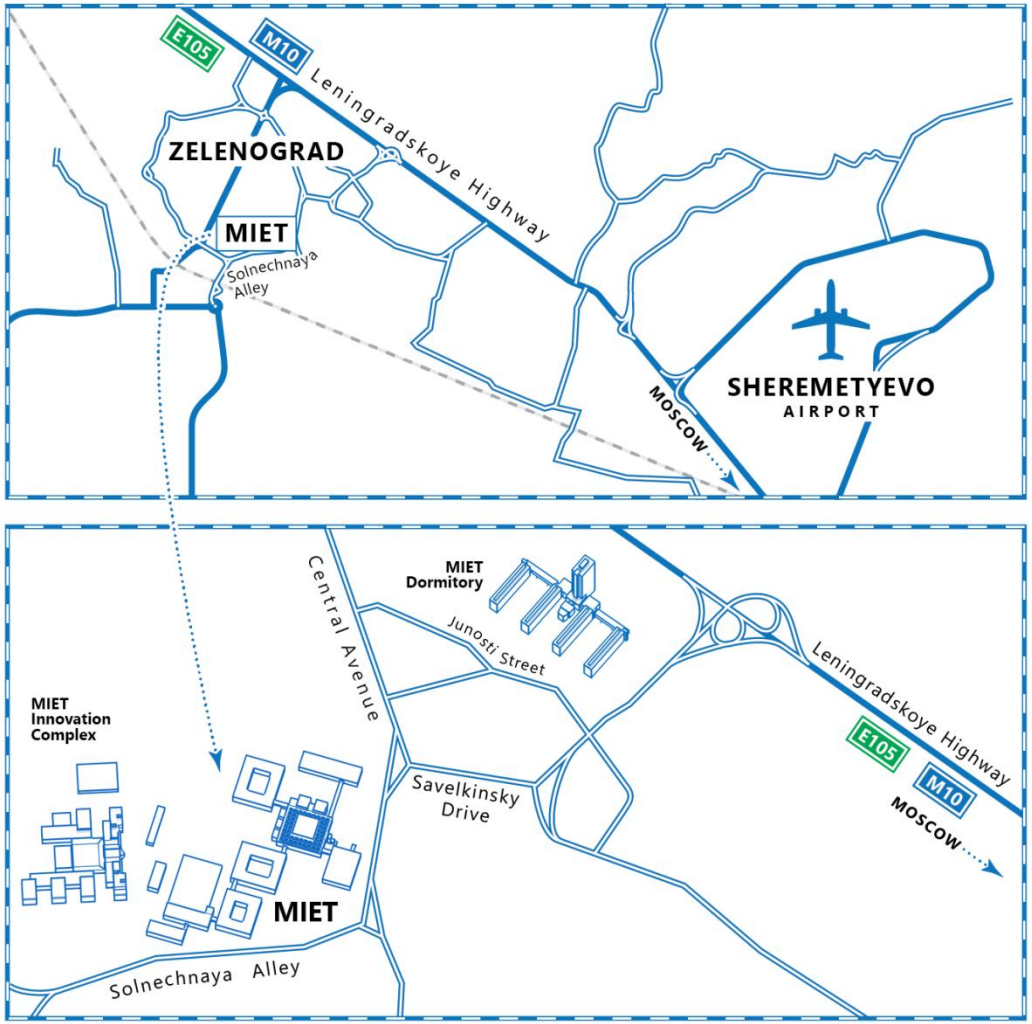

- literally “green town”
- location: 20 km northwest of Moscow
- founded 1958
- center of the microelectronics industry
- free economic zone
- innovations-oriented manufacturers

MIET in Brief

STAFF

1500 employees

450 Teachers

550 Researchers

100 Full professors

300 PhDs

5500 Students

400 Doctoral & postgraduate students

>1000 Annual graduates

MIET Research Activities

- Fundamental research in mathematics, physics, chemistry and electronics;
- Information technologies and telecommunications;
- Materials for micro-, nano- and optoelectronics;
- Micro- and nanoelectronic devices;
- Microsystem technology;
- Devices of fiber and integrated optics;
- Information control systems and complexes;
- Microelectronic radio systems and devices;
- Ecology and human life-support systems;
- Economics, management and marketing;
- Social and philosophical problems of science and engineering;
- Problems of general and professional education.

Synthesis of new functional nanomaterials

Nanoporous/nanotubular Anodic metal oxides and semiconductors

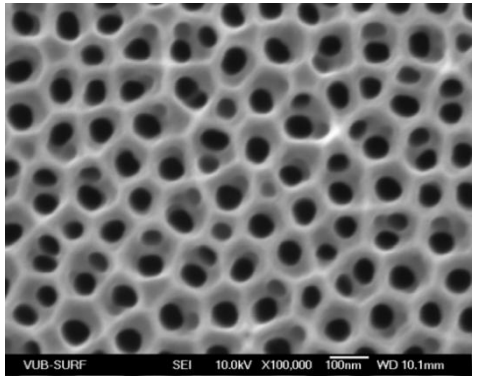

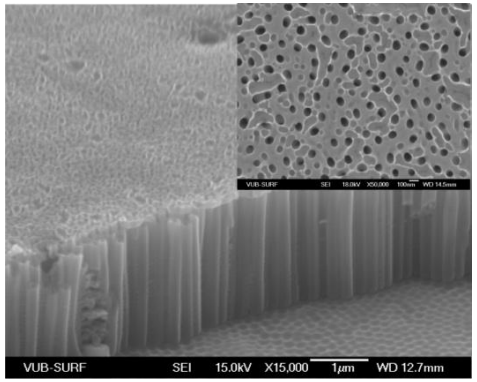

Thin films and nanoclusters

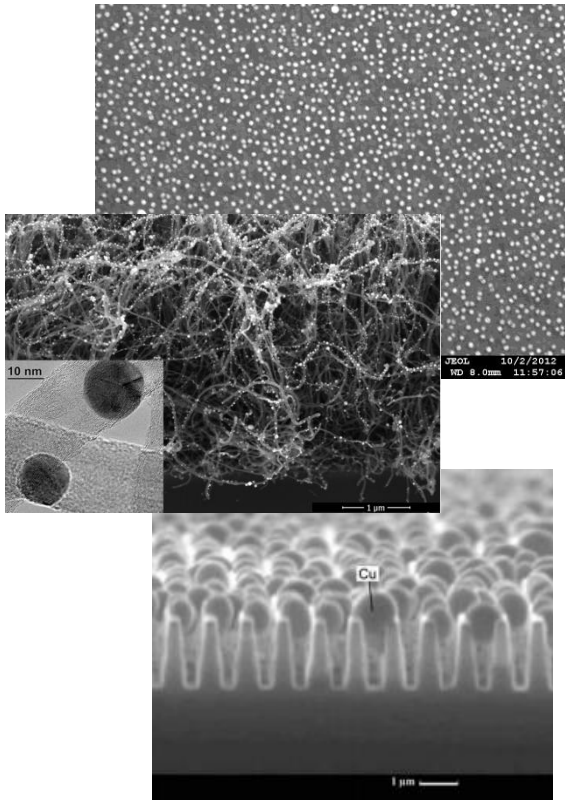

Nanotubes, Nanorods, Nanowires

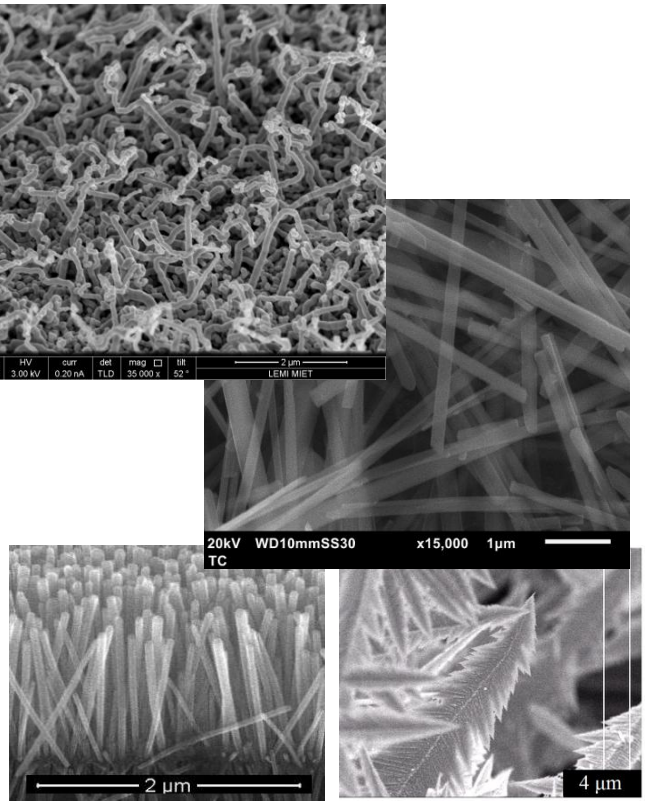

Application of metal nanoparticles

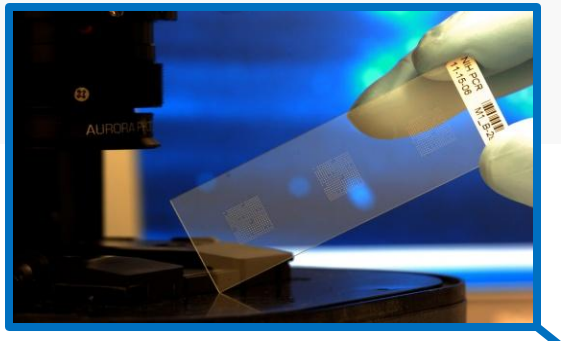

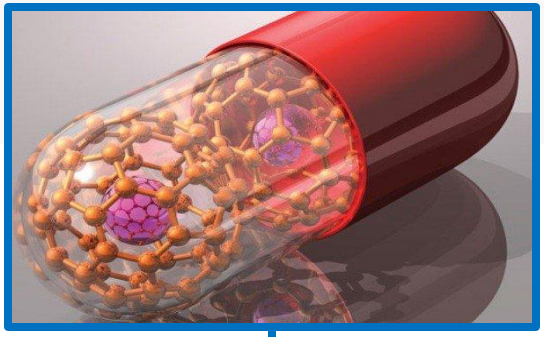

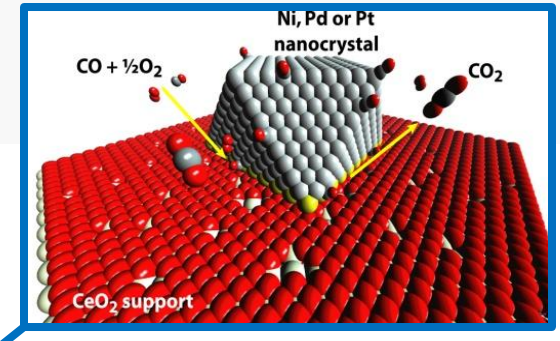

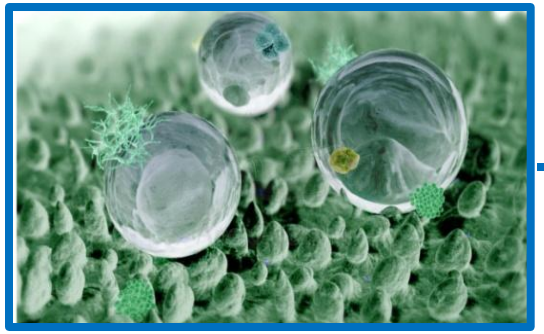

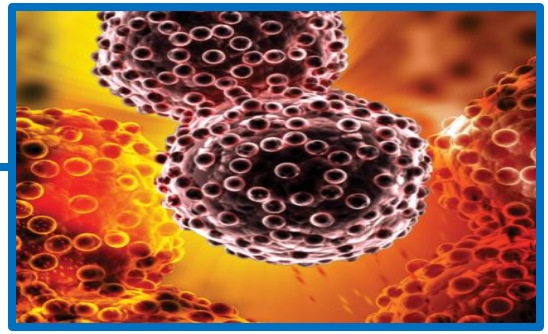

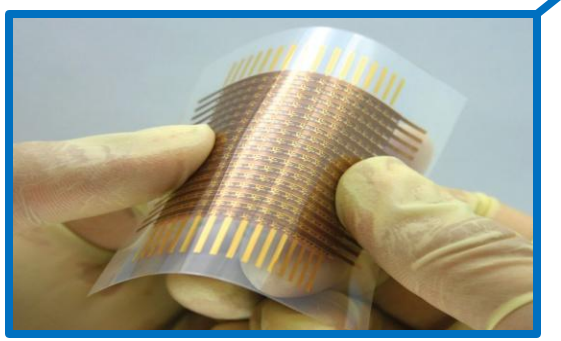

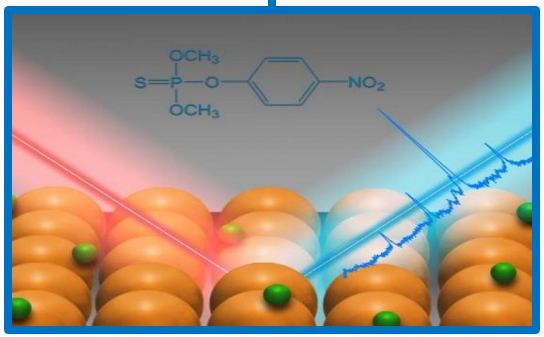

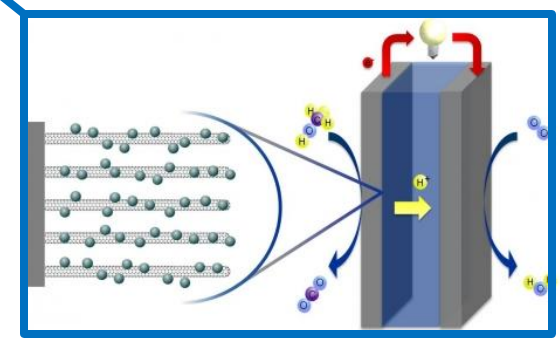

Surface-enhanced Raman scattering (SERS)

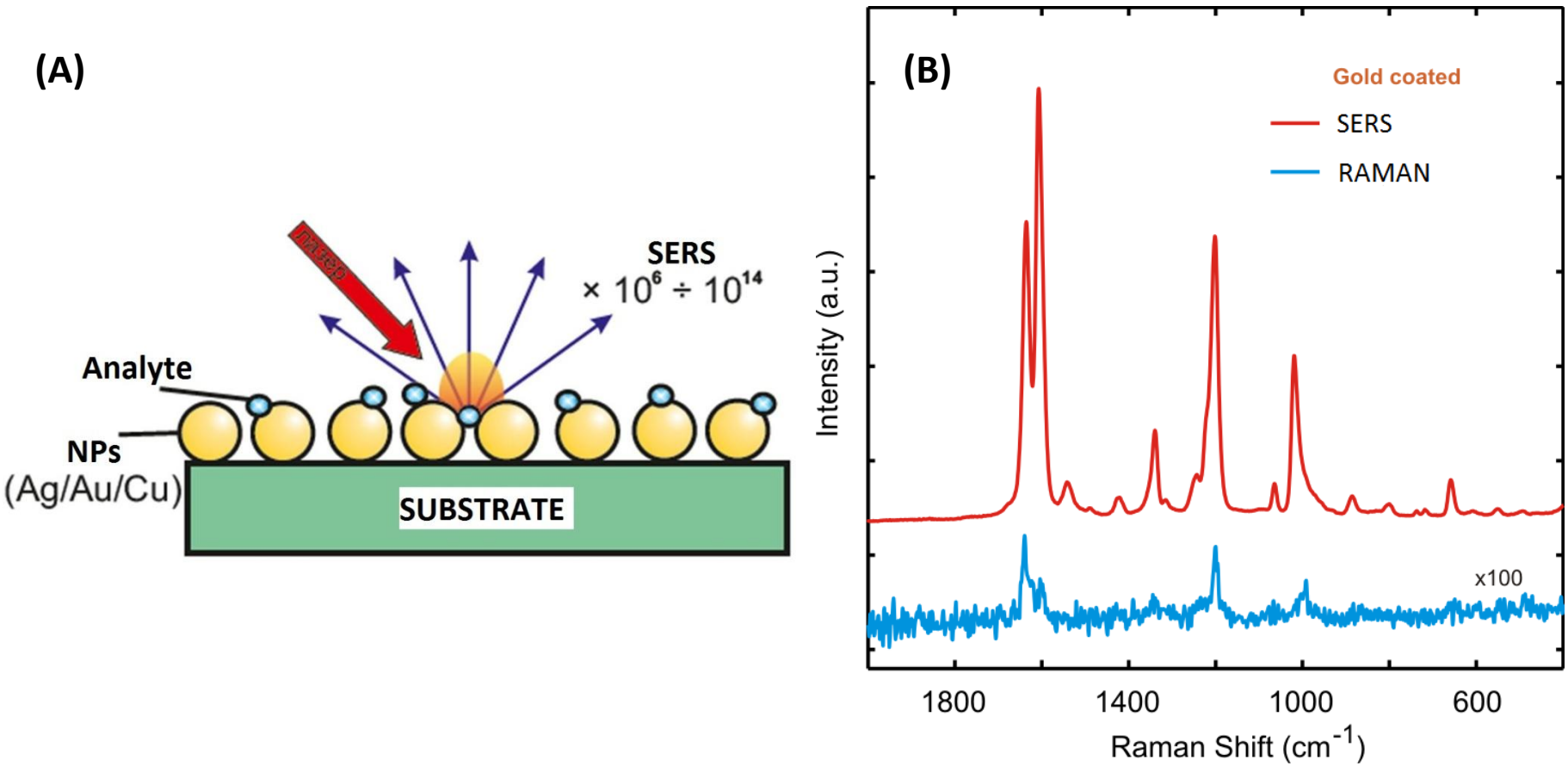

Schematic representation of the SERS effect (a) and comparison of the Raman spectra obtained in the presence and absence of gold nanoparticles (b)

Methods of forming nanoparticle arrays

Chemical liquid methods

- surface contamination of nanoparticles;
- low reproducibility of arrays;
- heterogeneity of the distribution of particles on the surface.

Electron beam lithography

- high labor intensity and cost

(a) $K_{SERS} \leq 10^4$

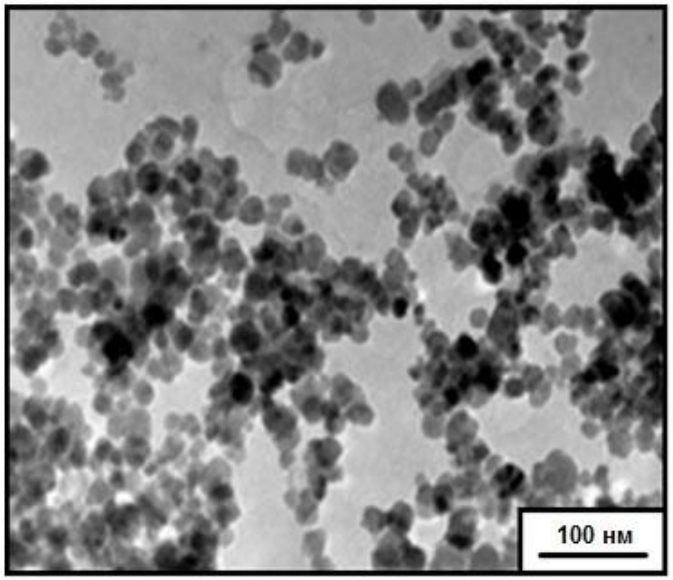

(b) $K_{SERS} \leq 10^{12}$

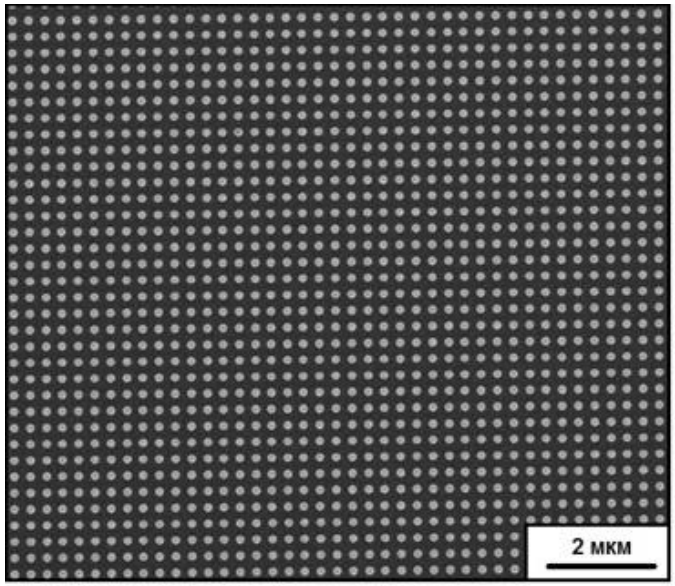

TEM image of a cluster of Fe3O4 (a) nanoparticles obtained by deposition from a colloidal solution on a solid surface [1], SEM image of an array of gold disks (b) formed using electron beam lithography [2]

[1] Zhaoyang Tong, et al. Sensors. – 2016. – V. 16. – P. 308.

[2] Madsen S., et al. Microscopy and Microanalysis. – 2013. – Vol. 19. – P. 1554-1555.

Vacuum thermal evaporation

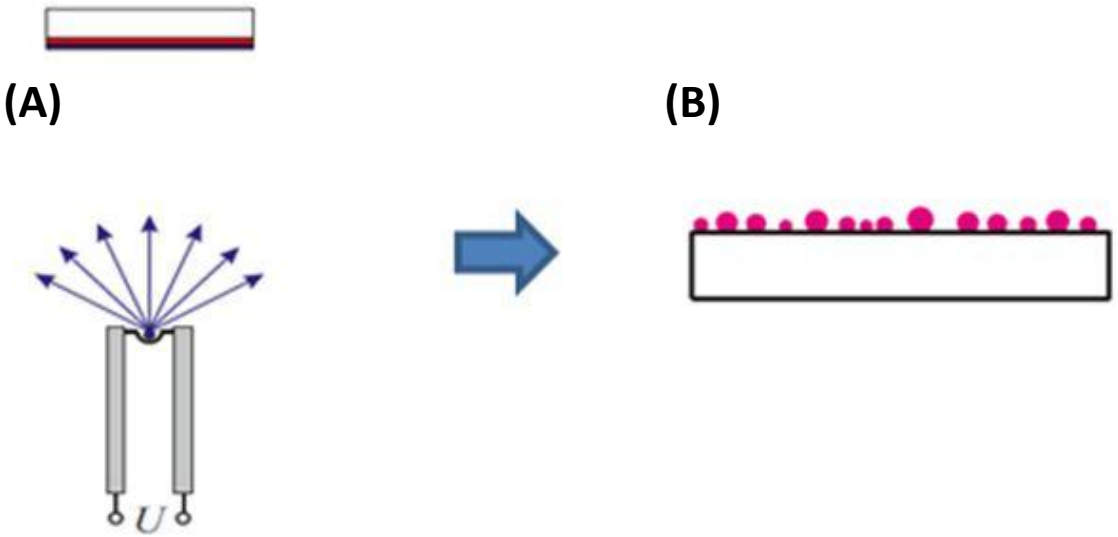

Schematic description of the formation of nanoparticle arrays by vacuum thermal evaporation.
A - deposition of material; **B** - vacuum annealing

What arrays we can form:
Silver (Ag), gold (Au), copper(Cu), nickel (Ni), bismuth (Bi), iron (Fe), antimony(Sb) and alloys of these components, e.g. Ag-Cu, Ag-Au etc.

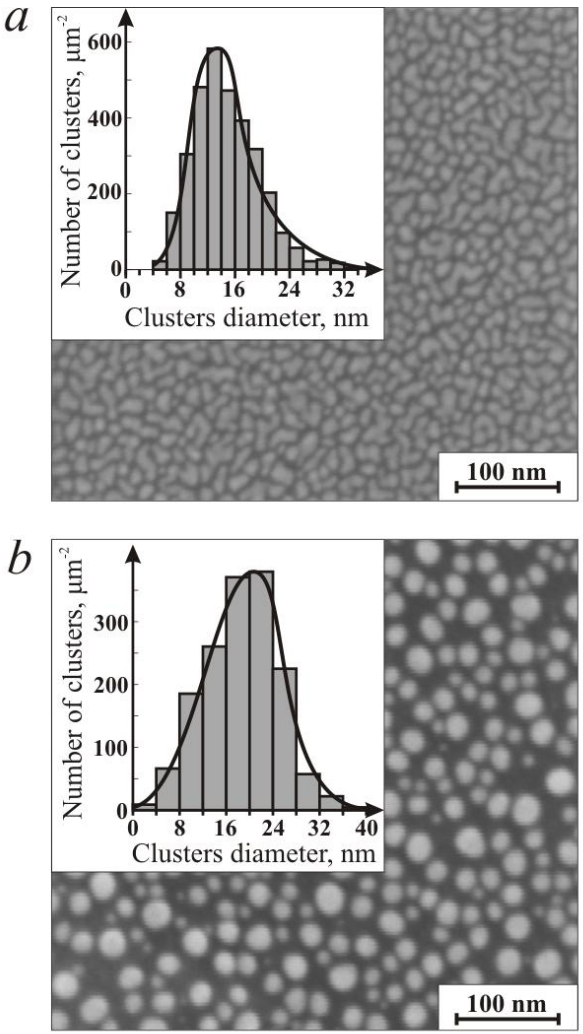

Silver nanoparticles: (a) 16 nm; (b) 21 nm

Au nanoparticle arrays of various average size

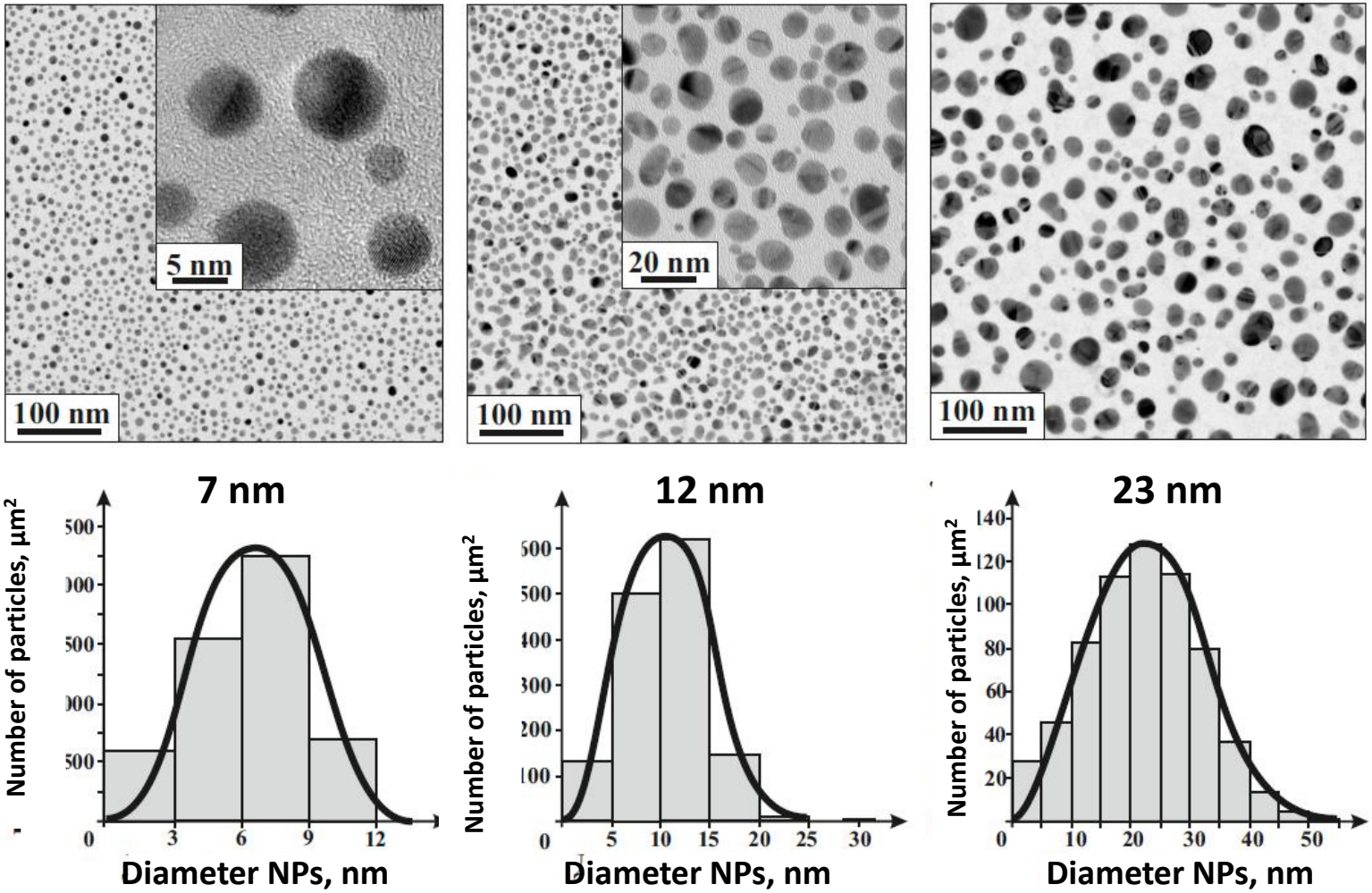

TEM micrographs of gold nanoparticles with different geometrical parameters of arrays and corresponding histograms of particle size distribution

Depending position plasmon resonance on geometrical parameters arrays Ag and Au

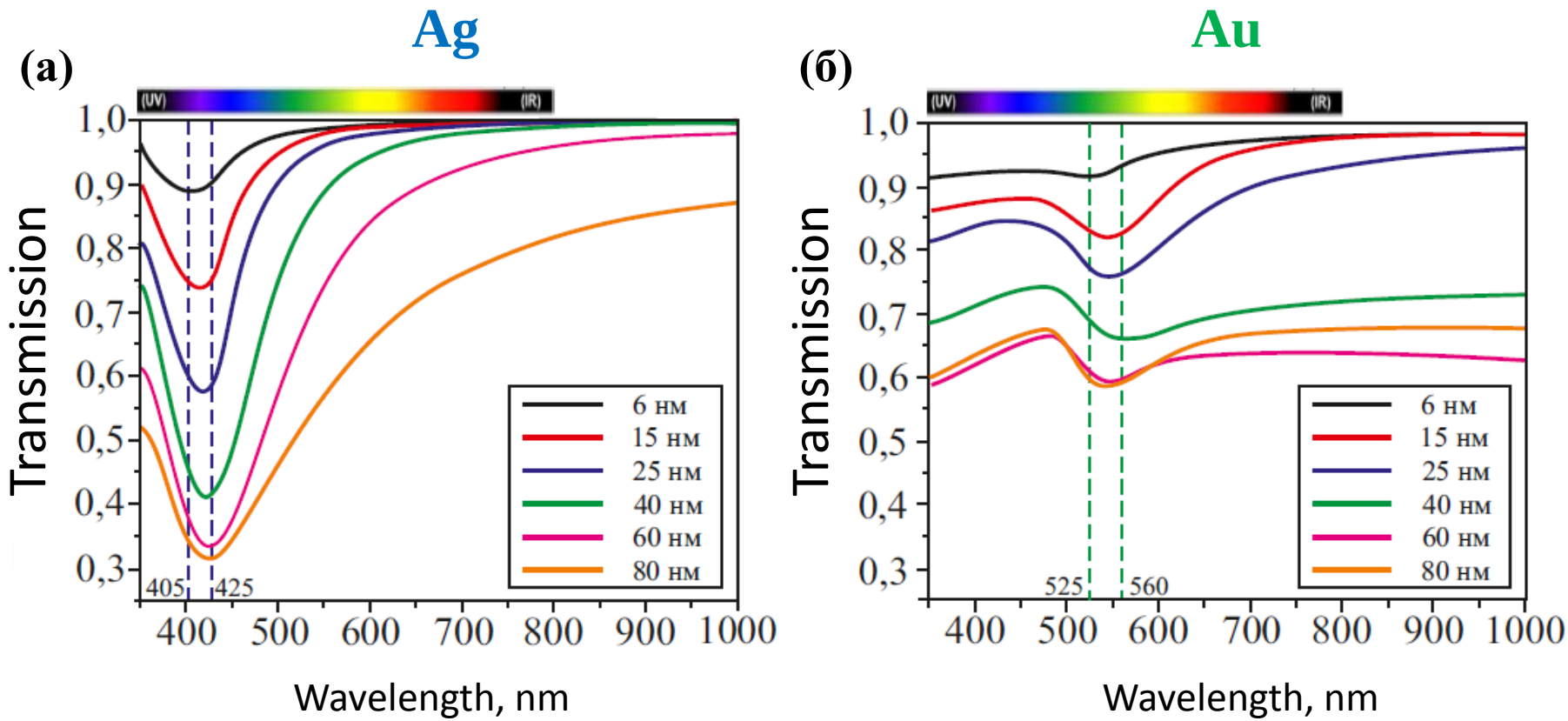

Transmission spectra of arrays of Ag (a) and Au (b) nanoparticles formed on glass with different average particle sizes

Formation of Au-Ag alloys nanoparticles

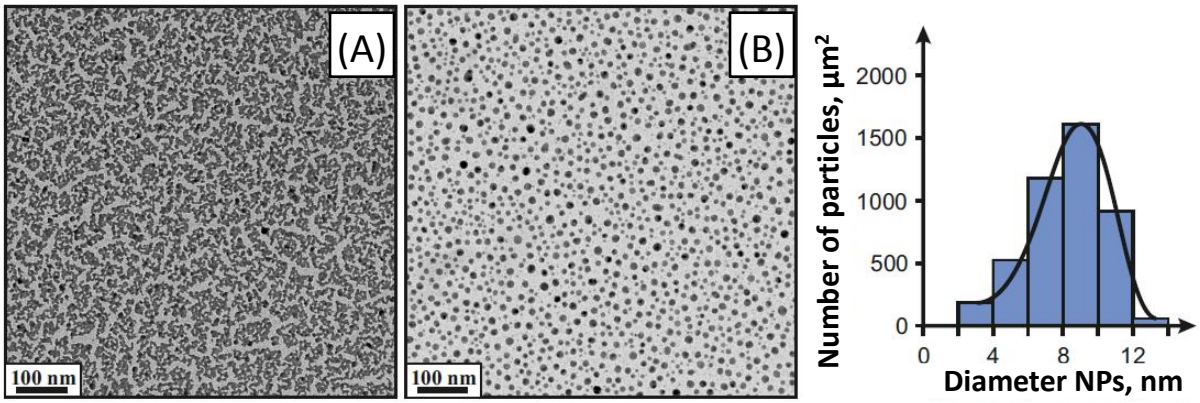

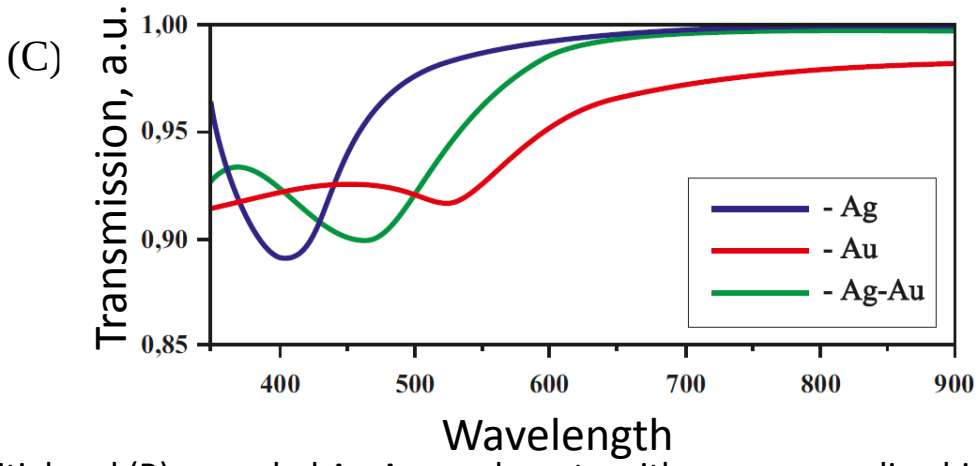

TEM images of (A) initial and (B) annealed Ag-Au condensate with a corresponding histogram of particle size distribution (weight portions of Ag — 0.6 mg; Au — 1.5 mg);
(C) Transmission spectra of (in) Ag, Au and AgAu arrays of nanoparticles (diameter ~ 9 nm);

Planar SERS substrate. The object of study is amorphous carbon (a-C)

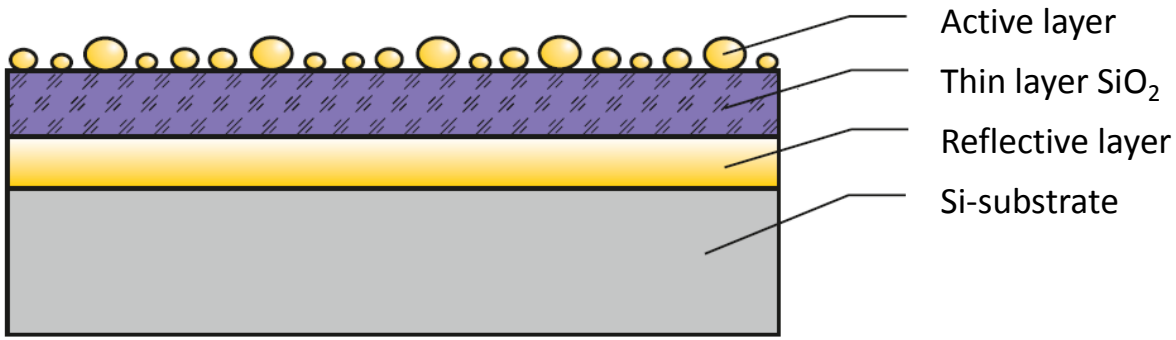

SERS substrate design scheme

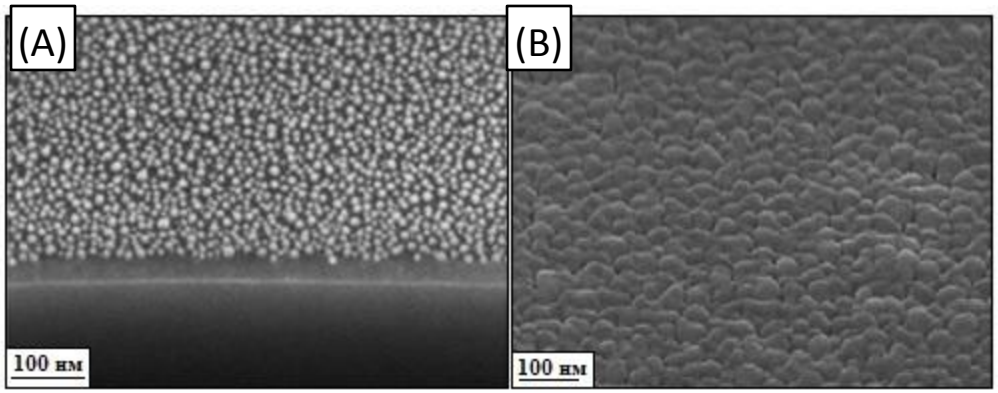

SEM images of the surface of the SERS substrate before (A) and after (B) the deposition of a layer of amorphous carbon

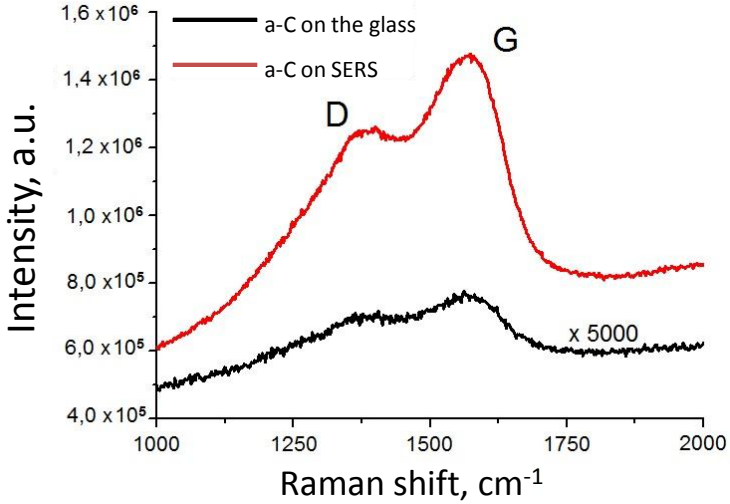

Raman spectra of amorphous carbon films (~ 25 nm) on glass and on a SERS substrate at λL = 488 nm

Ag-Cu composite nanoparticles

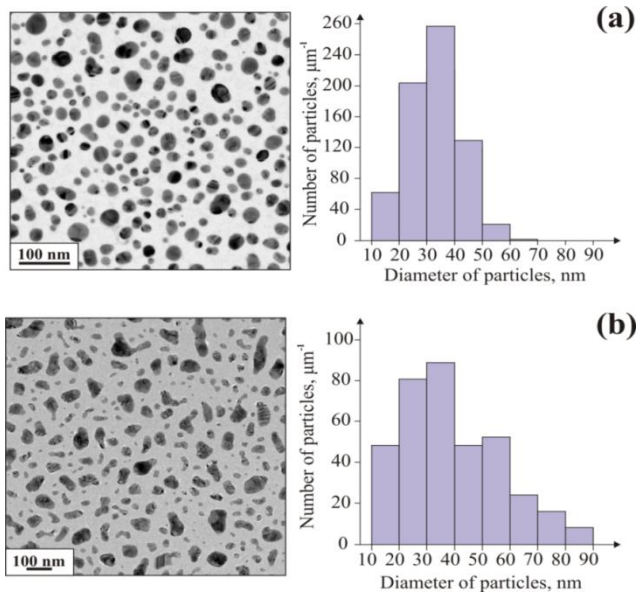

Fig.1. TEM images and particles size distribution histograms of silver (a) and Ag-Cu (b) nanoparticles arrays.

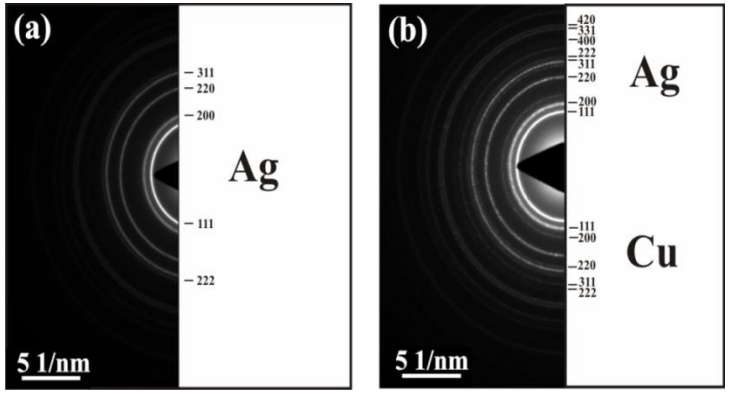

Fig.2. Selected area diffraction patterns of silver (a) and Ag-Cu (b) nanoparticles arrays.

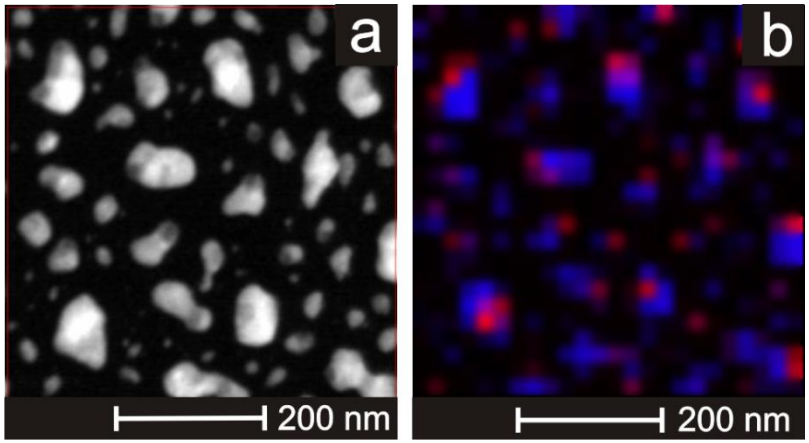

Fig.3. Fragmented STEM image of the studied array of nanoparticles (a); EDX elemental maps of this fragment (b), where copper is shown in red and silver in blue.

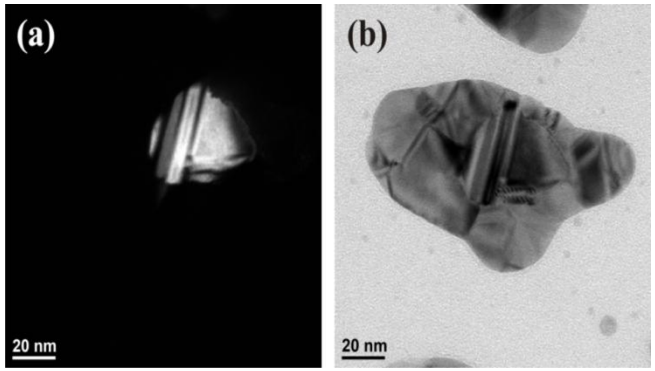

Fig.4. Dark field TEM image of Ag-Cu particle. To build this image the diffracted beam corresponding to (200) planes of copper lattice was used. (b) Bright field image of the same particle

SERS structures based on arrays of Ag, Cu and Ag-Cu

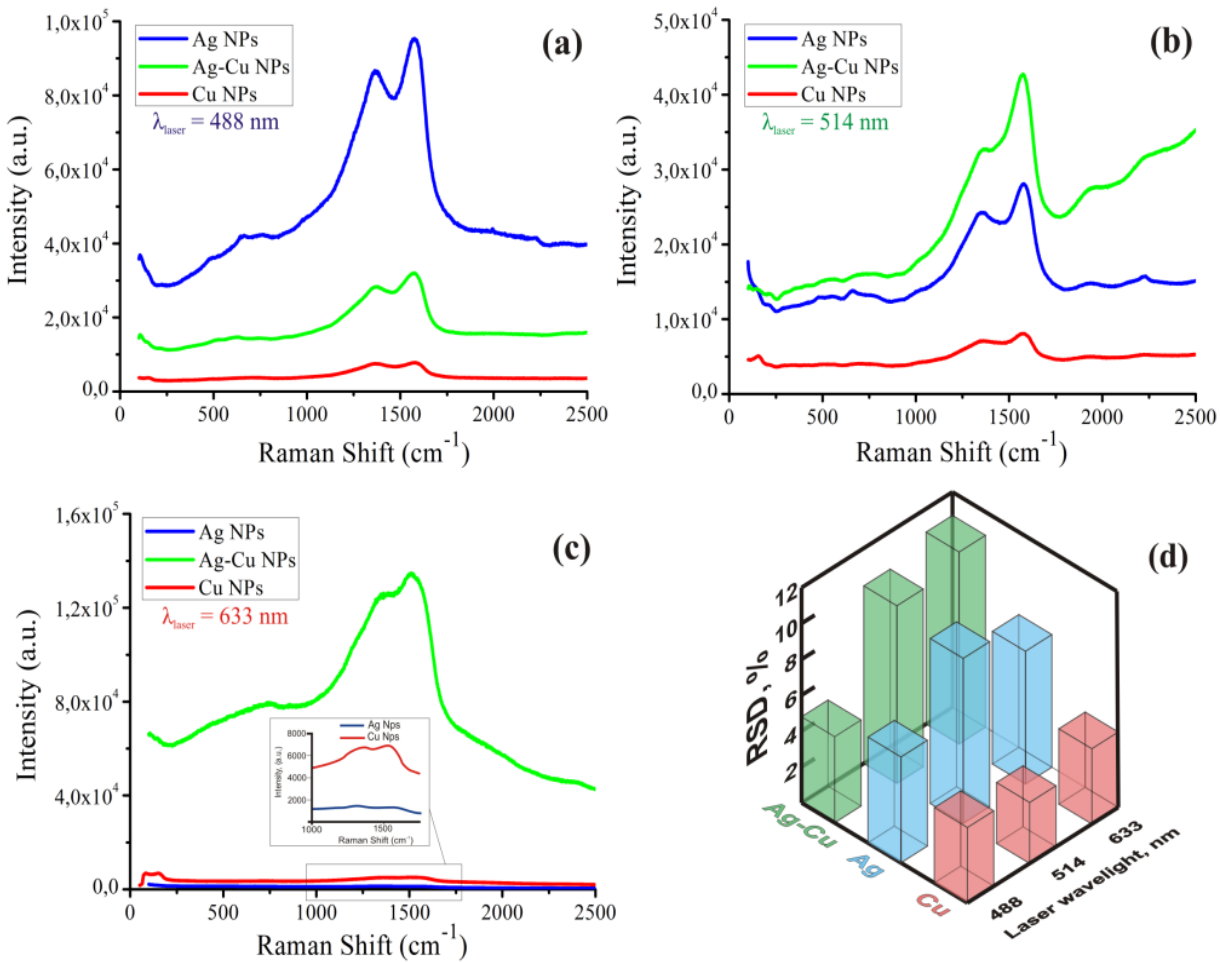

Raman spectra of amorphous carbon thin films deposited on SERS structures based on arrays of Ag, Cu and Ag-Cu nanoparticles using lasers with the wavelengths of 488 (a), 514 (b) and 633 nm (c); reproducibility of the SERS intensities for a-C film (1580 cm^{-1}) on Ag, Cu и Ag-Cu NPs SERS substrate. The histogram shows the estimated RSD values (d).

Detection of µM Trimethylamine N-oxide

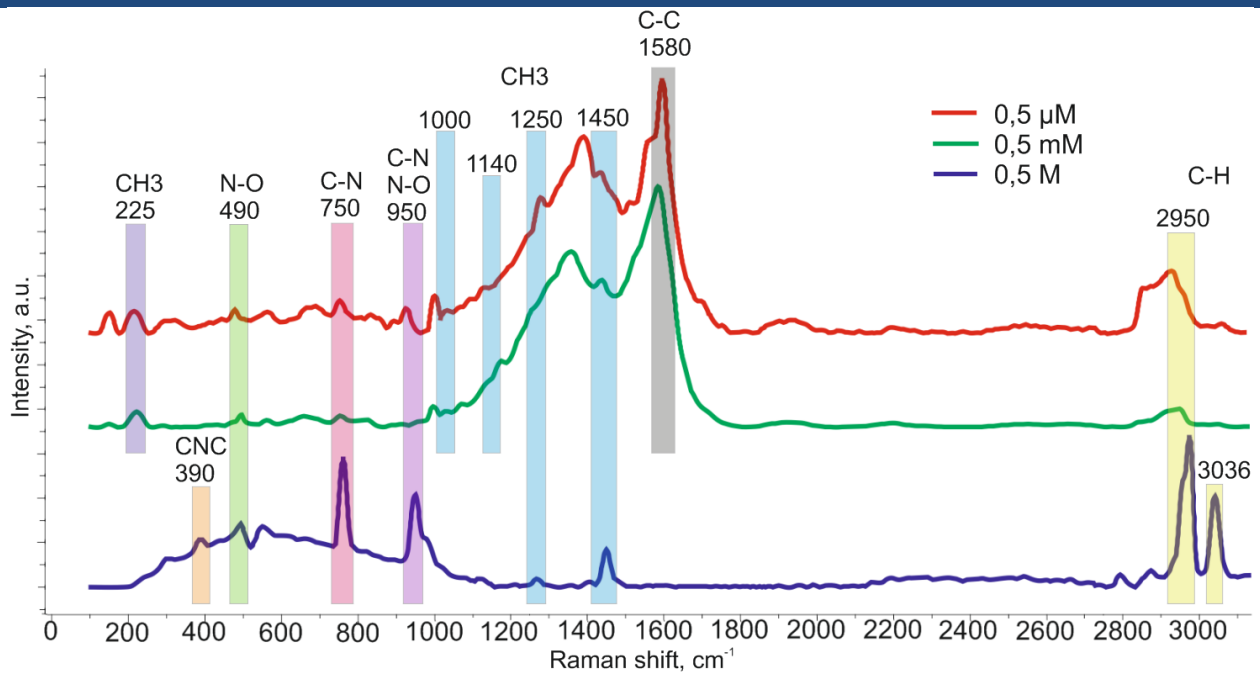

Raman spectra of 0.5 µM, 0.5 mM and 0.5 M of TMAO at wavelength of 514 nm on the structure of Si \Ag\SiO2\Ag

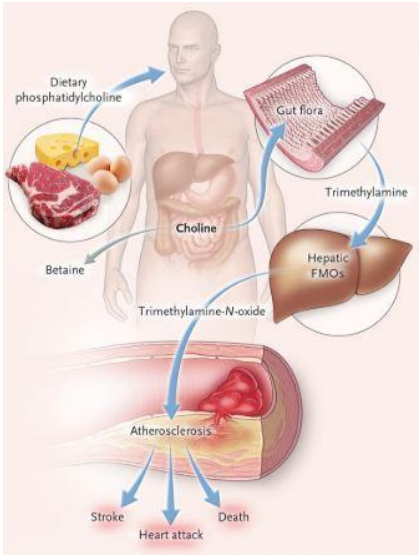

Scheme of TMAO formation in the body

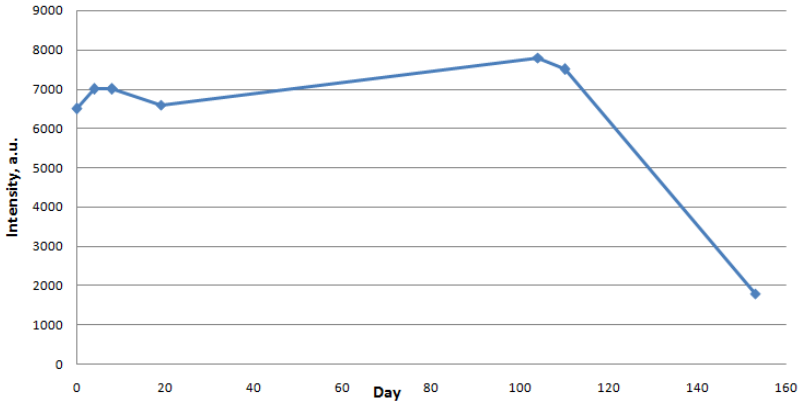

SERS substrate lifetime

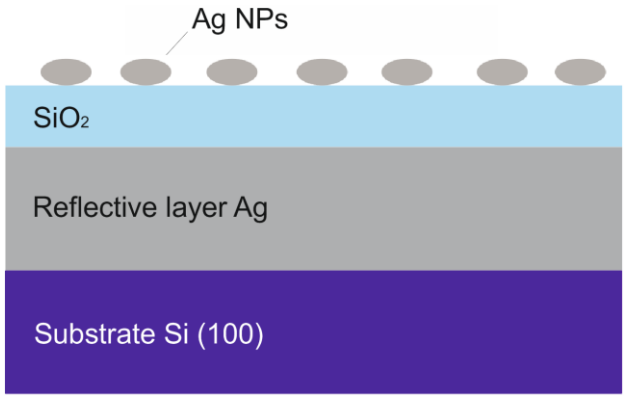

SERS Scheme

Detection of TMAO in human blood and plasma

band type	Munroe et al.	TMAO µM	TMAO mM	TMAO M	Plasma	Blood
CH3 torsion	225	220	220	-	220	219
CH3 torsion	293	295	295	-	300	296
CNC bend	386	-	-	390	400	
N-O stretch	489	480	465	490	487	490
C-N stretch	764	755	760	760	760	750
N-O stretch	945	930	960	950	-	-
C-N stretch	945	930	960	950	-	-
CH3 def	1000	1005	1010	-	1005	996
CH3 rock	1136	1130	1155	-	1150	1126
CH3 rock	1231-1268	1280	1250	1270	1250	1226
CH3 def	1400-1465	1430	1460	1450	1450	1467
C-H stretch	2931-2952	2930	2930	2955	2935	2927
C-H stretch	3036	3060	-	3040	3066	3060

Comparison of the literature peaks of TMAO and the corresponding experimental peaks

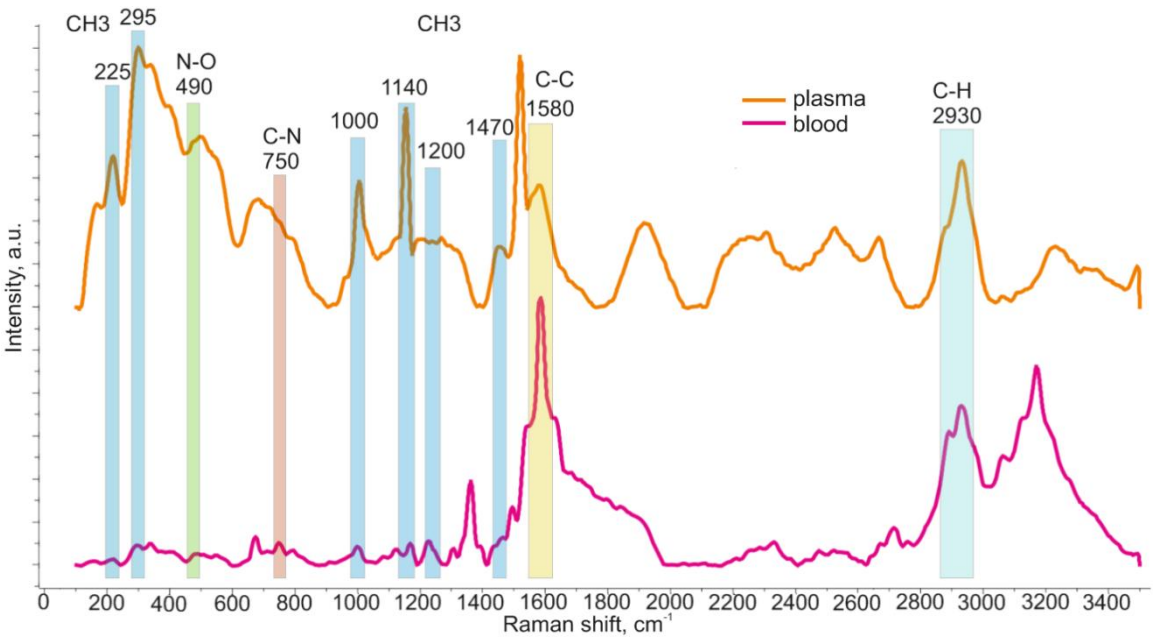

Raman spectra of human blood and plasma at wavelength of 514 nm on the structure of Si \Ag\SiO2\Ag

Photosynthesis

The use of plasmonic nanoparticles in the composition of the catalyst may allow the use of "free" solar energy for:
- Water purification
- Processing of co2 into methanol, methane
-Decomposition of water into oxygen and hydrogen
- Decomposition of exhaust gases of an internal combustion engine

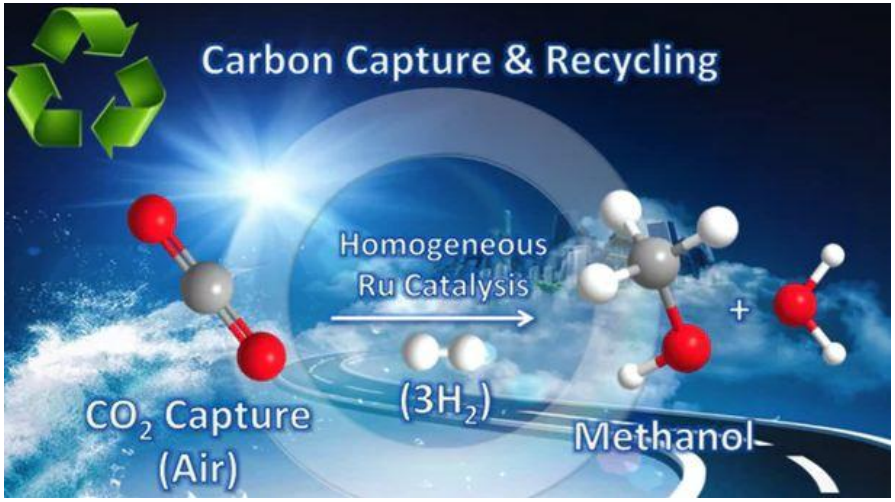

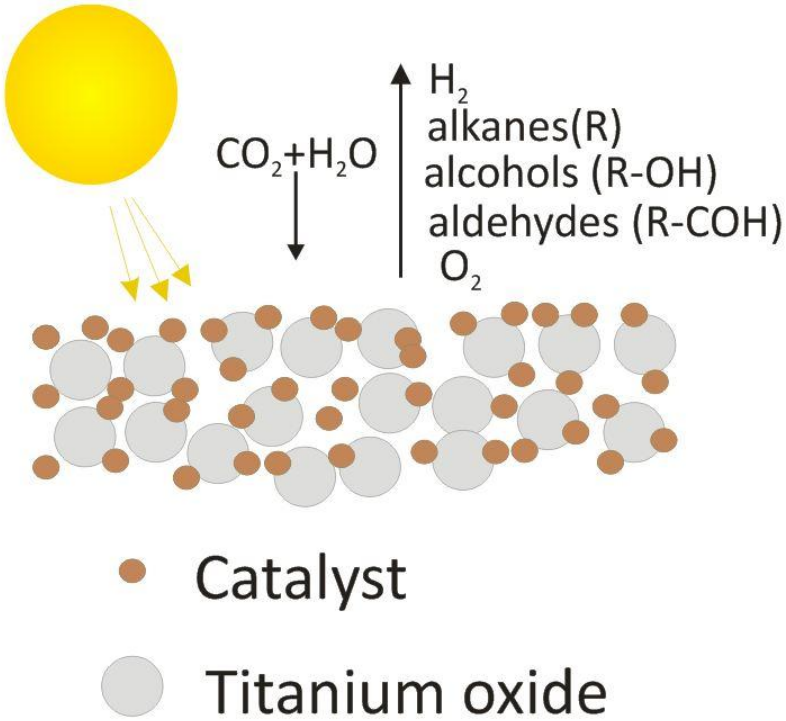

$$CO_2 + 3H_2 = CH_3OH + H_2O$$
$$CO_2 + H_2 = CO + H_2O$$
$$CO + 2H_2 = CH_3OH$$

Catalytic systems

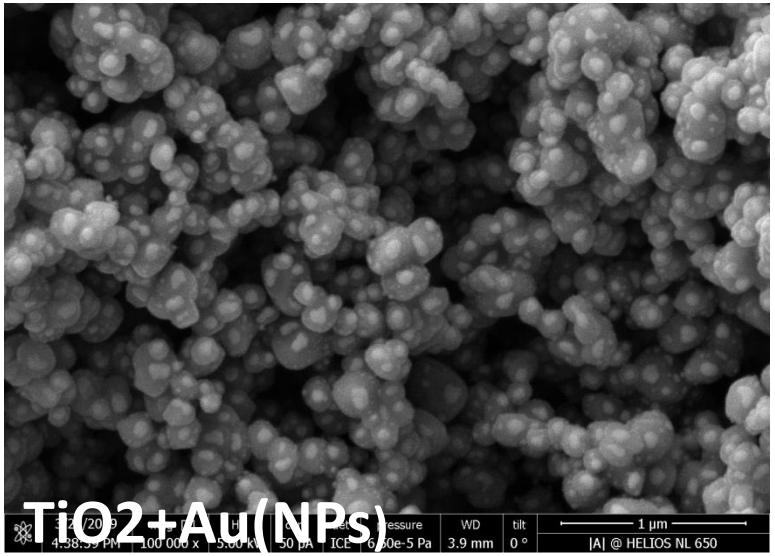

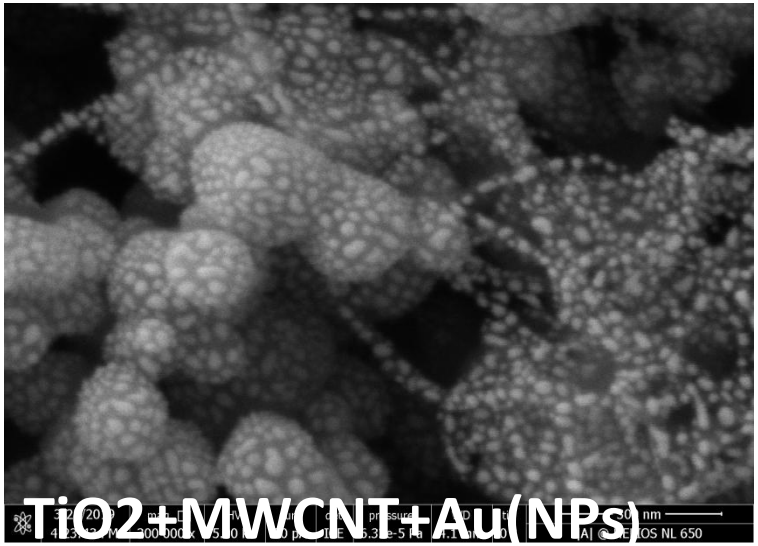

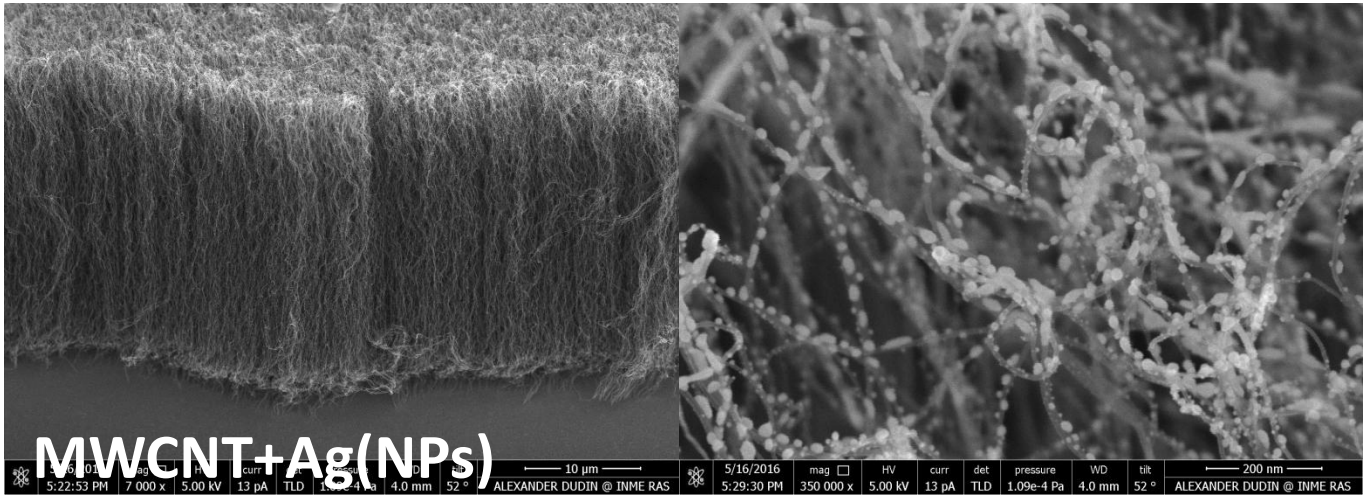

IR spectra of TiO2 with Au and Ag particles exposed to UV

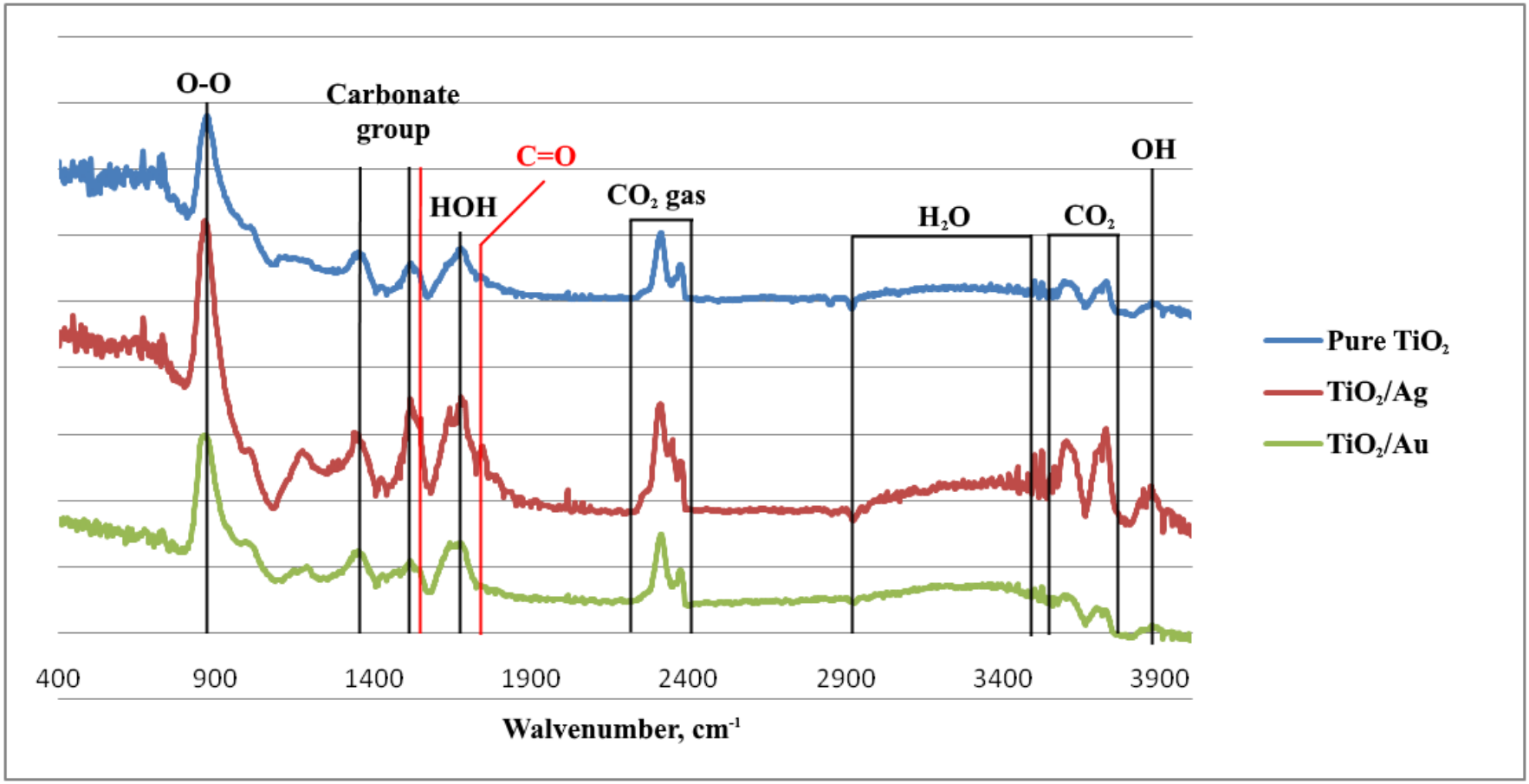

The photocatalytic activity of TiO2-based catalyst

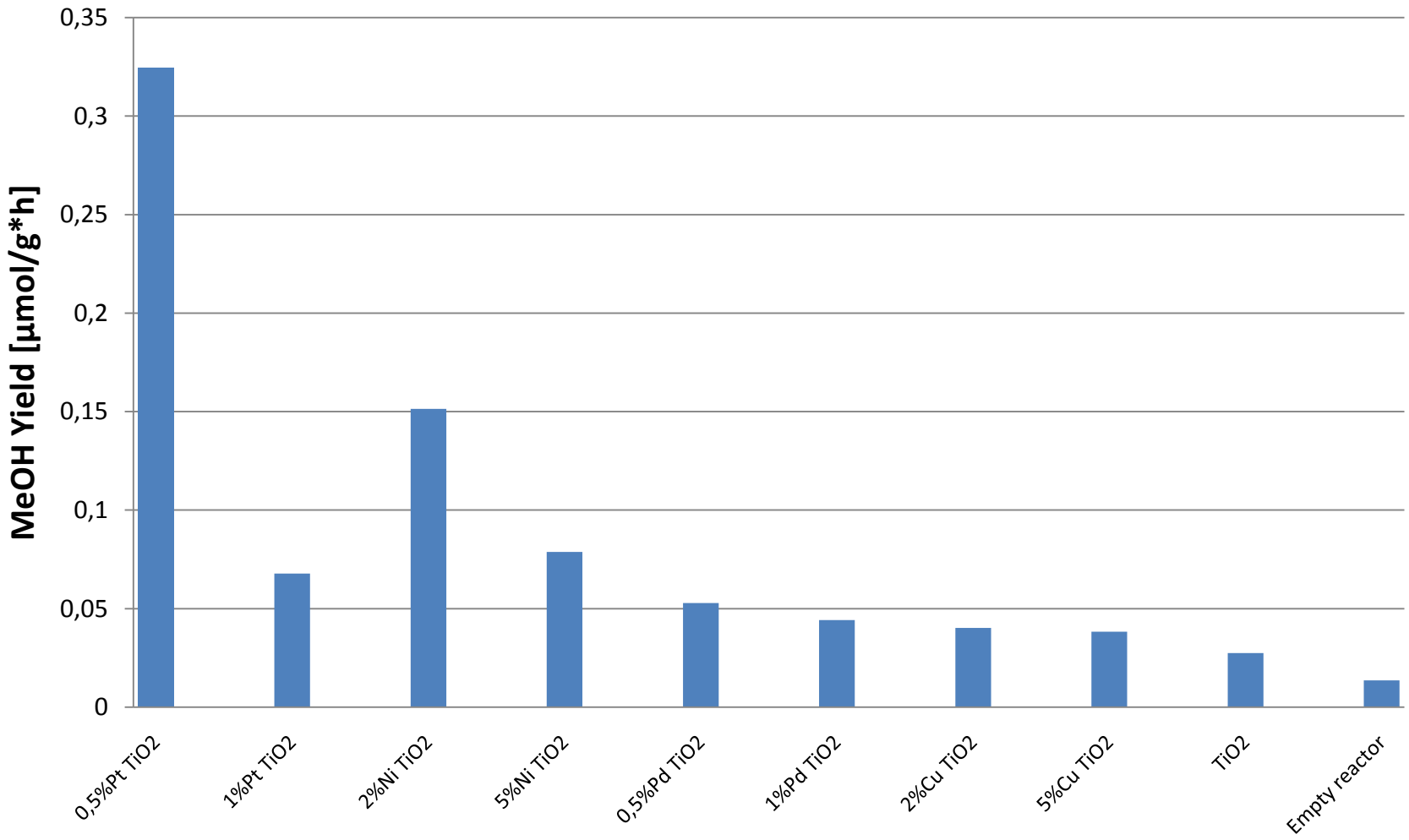

Articles used for presentation

[1] S.V. Dubkov, A.I. Savitskiy, A.Y. Trifonov, G.S. Yeritsyan, Y.P. Shaman, E.P. Kitsyuk, A. Tarasov, O. Shtyka, R. Ciesielski, D.G. Gromov, SERS in red spectrum region through array of Ag–Cu composite nanoparticles formed by vacuum-thermal evaporation, Optical Materials: X. 7 (2020). https://doi.org/10.1016/j.omx.2020.100055. (IF=2.77, Q1)

[2] S. Dubkov, D. Gromov, A. Savitskiy, A. Trifonov, S. Gavrilov, Alloying effects at bicomponent Au-Cu and In-Sn particle arrays formation by vacuum-thermal evaporation, Materials Research Bulletin. 112 (2019) 438–444. https://doi.org/10.1016/j.materresbull.2018.10.003. (IF=4.019, Q1)

[3] D.G. Gromov, S.V. Dubkov, A.I. Savitskiy, Y.P. Shaman, A.A. Polokhin, I.A. Belogorokhov, A.Y. Trifonov, Optimization of nanostructures based on Au, Ag, Au[sbnd]Ag nanoparticles formed by thermal evaporation in vacuum for SERS applications, Applied Surface Science. 489 (2019) 701–707. https://doi.org/10.1016/j.apsusc.2019.05.286. (IF=6.182, Q1)

[4] O. Shtyka, R. Ciesielski, A. Kedziora, W. Maniukiewicz, S. Dubkov, D. Gromov, T. Maniecki, Photocatalytic Reduction of CO2 Over Me (Pt, Pd, Ni, Cu)/TiO2 Catalysts, Topics in Catalysis. 63 (2020) 113–120. https://doi.org/10.1007/s11244-020-01241-y. (IF=2.406, Q1)

This work was financially supported by the grant of President of the Russian Federation (project MK-2222.2019.8) and by the Russian Science Foundation (Project No. 19-19-00595)

ME IN R^G

Thanks For Your Attention